ARTICLES

Time-Resolved Molecular Beam Mass Spectrometry of the Initial Stage of Particle Formation in an Ar/He/C_2H_2 Plasma

J. Benedikt,* A. Consoli, M. Schulze, and A. von Keudell

Arbeitsgruppe Reaktive Plasmen, Ruhr-Universität Bochum, 44780 Bochum, Germany

Received: April 13, 2007; In Final Form: June 21, 2007

The temporal evolution of the neutral plasma chemistry products in a capacitively coupled plasma from argon/helium/acetylene is followed via molecular beam mass spectrometry with a time resolution of 100 ms. Several chemistry pathways are resolved. (i) The formation of $C_{2n}H_2$ ($n = 2-5$) molecules proceeds via the following sequence: the production of highly reactive C_2H radicals in electron impact dissociation of C_2H_2 is followed by C_2H induced chain polymerization of $C_{2n}H_2$ ($n = 1-4$). (ii) C_nH_4 ($n = 4, 5, 6$) compounds are detected already at an early stage of the discharge excluding polymerization reactions with C_2H radical being responsible for their formation. Instead, vinylidene reactions with acetylene or mutual neutralization reactions of ionic species are proposed as sources of their formation. (iii) Surface reactions are identified as the source of C_8H_6. The measured hydrocarbon molecules represents possible precursors for negative ion formation via dissociative electron attachment reactions and can hence play a crucial role in particle nucleation. On the basis of the comparison of our data with available experimental and modeling results for acetylene plasmas in the literature, we propose $C_{2n}H_2$ ($n > 1$) molecules as important precursors for negative ion formation.

Introduction

The generation of nanoparticles in reactive plasmas is a vivid area of research.[1,2] Plasma-produced particles can be used for nanoparticle-based transistors or luminescence devices,[3] for stress release in nanocomposites[4] or for improving electrical properties of hydrogenated amorphous silicon.[5] The production of especially small particles is of key interest for many applications, since finite size or quantum effects can be exploited for high value products. The production of larger particles is in general more efficiently performed via standard chemistry routes.

Small particles are inherently formed in many reactive plasmas using various source gases such as silane or acetylene. Particle nucleation in low-pressure plasmas is still not completely resolved, but it is most probably initiated by negative ions.[1] These negative ions stay confined in the plasma volume due to the confining sheath potential between plasma and surrounding walls. Negative ions undergo successive ion−molecule reactions at a considerable rate leading to the formation of very large macromolecules. At a critical size of approximately 1−2 nm, charge fluctuations occur, since ion and electron fluxes onto a particle from the plasma can balance. During these charge fluctuations individual particles do not repel each other anymore and they may coalesce in a so-called nucleation burst: in a very short time period a large number of small particles agglomerates to form larger nanoparticles with sizes larger than 50 to 100 nm. In this size range, the balance between electron flux and ion flux onto the particles causes them to stay negative with respect to the plasma potential, similar to a floating probe. They grow further via attachment of neutral radicals at the particle surface. Because of this negative charge, particles stay confined in the plasma unless they are extracted by strong electric fields or simply by gravity, if the particles become very large.

In our previous experiments the particle formation in a combination of an capacitively (CCP) and inductively (ICP) coupled plasma has been investigated. In a two step procedure, particles are generated at first by injecting acetylene in an argon/helium CCP plasma. Then the plasma is switched externally into the ICP mode while the particles stay confined. The interplay between particles and plasma performance in the ICP mode causes various instabilities as described previously.[6,7] The final particle size is dominated by the initial particle generation phase during the injection of acetylene in the argon/helium CCP plasma, with two nanometer particles being detected already 250 ms after plasma ignition.[8]

The most critical stage for particle formation is their nucleation, the transition phase between individual small molecules to macromolecules. Mass spectrometry is perfectly suited to follow this phase since a large number of different species is in principle accessible to this diagnostic. Deschenaux et al.[9,10] performed mass spectrometry measurements of neutrals and positive and negative ions in C_2H_2 CCP (pressure 10 Pa, C_2H_2 flow 8 sccm, RF power 40 W). The mass spectra indicate the preferential formation of hydrocarbon species with even number of carbon atoms. C_4H_2, $C_4H_2^+$, and C_6H^- are the species with highest signal intensities among neutral species (except C_2H_2), positive ions and negative ions respectively. Negative ions were measured in pulsed plasma with a frequency of 500 Hz in order to be able to extract them. This modulation resulted probably in slightly different plasma properties. These measurements can reveal the dominant plasma chemistry products, however, it is difficult to isolate different reaction pathways

10.1021/jp072892w CCC: $37.00
Published on Web 09/22/2007

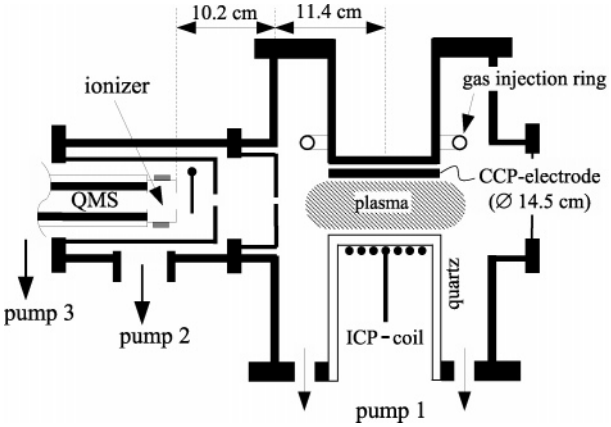

Figure 1. Experimental setup with implemented mass spectrometer.

leading to their formation. These pathways can be tested by coupling a plasma and a chemistry model. The hydrocarbon chemistry in acetylene containing CCP was modeled by de Bleecker et al.[11,12] Their self-consistent one-dimensional fluid model containing neutral, positive and negative species containing up to 12 carbon atoms could reproduce reasonably well main features of neutral species and positive ion mass spectra of Deschenaux et al. However, the number of reactive species and reactions that can be considered in any model is always limited (for example only $C_{2n}H^-$ anions were considered in this model), and many unknown reaction rates need to be estimated, providing unwanted freedom and uncertainty in the results. This uncertainty can only be resolved by comparison to experimental data.

In this work, we aim at revealing the chemistry pathways leading to formation of large hydrocarbon molecules by means of time-resolved molecular beam mass spectrometry measurements in an $Ar/He/C_2H_2$ CCP. These large molecules represent precursors for negative ion formation for example via dissociative electron attachment (DEA) reactions and can therefore be important for particle nucleation.

Experimental Methods

A sketch of the experimental setup is shown in Figure 1. The reactor chamber is similar to a GEC reference cell, with an extended reactor height and electrode spacing of 6 cm. The plasma can be driven inductively from the bottom side by an external coil and capacitively from the top side by a planar electrode. A movable substrate holder is embedded in the capacitively driven electrode. A silicon wafer is mounted in the holder, which is then loaded into the reactor via a load lock. The dielectric window for the inductive coupling is a dome shaped quartz cylinder, which avoids losses of the rf power due to the generation of eddy currents in any metallic parts nearby the ICP-coil. All gases are injected via a ring shower surrounding the capacitively driven electrode.[6,7] The reactor chamber is pumped by a turbomolecular pump. A butterfly valve, which is mounted in the pump line, is used for pressure control. The generation of particles in the plasma is performed via the scheme depicted in Figure 2a: First (i), a flow of argon and helium as buffer gas is set to 4 sccm (argon) and 15 sccm (helium) at a pressure of $p = 4$ Pa. In addition, an acetylene flow of 4 sccm is added; then (ii) the capacitively driven electrode is used to strike the plasma at a forward power of 80 W for a time period $\Delta t_1 = 8$ s; afterward (iii), the acetylene flow is switched off. The total gas pressure prior to the plasma ignition is 6 Pa and decreases to 4.4 Pa after the plasma is ignited and the acetylene flow is turned off. The butterfly valve is kept at a fixed position

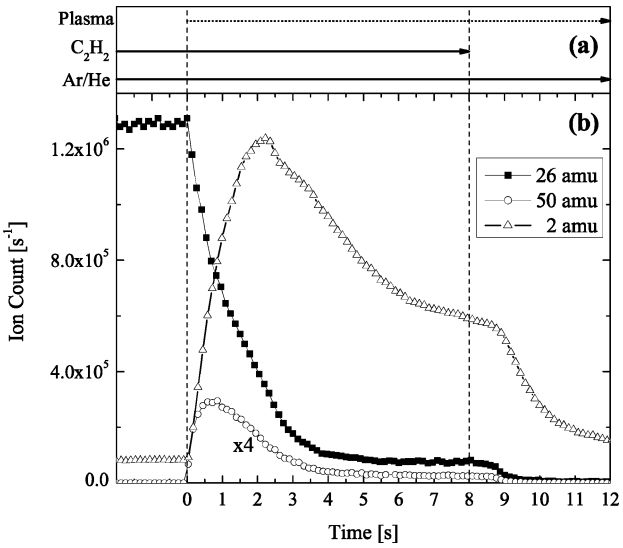

Figure 2. Course of the experiment (a) and measured signals at masses 2, 26, and 50 amu (b).

at all times. The residence time of the neutral species under the plasma off conditions is 4.9 s. It was shown, that the initial density of a precursor gas in the volume surrounding the plasma can strongly influence the plasma process and dust particle formation.[13,14] To control this effect, it is checked prior to every experiment by mass spectrometer to see that acetylene has reached its steady-state density. The neutral plasma chemistry is followed in time using molecular beam mass spectrometry. A Balzers HiQuad mass spectrometer QMG 700 with a mass range up to 2048 amu is mounted inside a two-stage differential pumping system. The sampling orifice has a diameter of 0.6 mm and is at a distance of 114 mm from the reactor axis and 41 mm from the edge of the electrode [cf. Figure 1]. The line of sight distance between the first orifice and the ionizer in the mass spectrometer is 102 mm. The base pressure in the mass spectrometer is 2×10^{-8} mbar and around 3×10^{-7} mbar during the measurements. A mechanical flag is mounted directly in front of the ionizer in the second stage to allow a separate measurement of the background signal without the molecular beam component. This flag is manipulated externally via a mechanical feedthrough. It is observed that the background signal is a constant fraction of the beam signal for the measurement of the neutral species selected in this work. Since only relative signals are compared, a background subtraction is not necessary prior to the data analysis.

The mass dependence of the transmission function of the mass spectrometer is calibrated using helium, neon, argon, krypton, xenon, nitrogen, and oxygen gases at known partial pressures, yielding: signal $\propto$ mass$^{-0.88}$. The ionizer of the mass spectrometer is set to a positive potential avoiding thereby the collection of positive ions. The axis of the mass spectrometer is tilted by 5° with respect to the axis of the extracted molecular beam in order to prevent UV photons from the plasma from reaching the secondary electron multiplier. Otherwise a UV photon induced background in the measured signals is observed.

The acquisition of an overview spectrum of all masses takes several tenths of seconds, which is longer than the time span for acetylene injection and particle generation. In order to achieve a better time resolution, a *step−scan* procedure is employed instead: first the variation of a signal at a selected mass (integration time 50 ms) is measured, together with a reference signal at mass 26 amu (C_2H_2 parent peak, integration time 10 ms) with good temporal resolution of about 100 ms

(250 ms for the signals at masses higher than 99 amu, where longer integration time of 100 ms are chosen) during a plasma experiment (*scan*). Afterward, the next mass channel is selected (*step*) and an identical plasma experiment with the same process parameters is repeated. The signal at mass 26 amu serves then as a reference signal and allows us to identify the exact moment of plasma ignition in different experiments. At the end, complete mass spectra at a given time after plasma ignition can be reconstructed, with a time resolution of 100 ms.

An example of two such steps measured at mass 50 amu (parent peak of C_4H_2 molecule) and at mass 2 amu (H_2) are shown in Figure 2b. The temporal evolution of the signal at mass 26 amu is identical in every measurement and proofs the reproducibility of the whole *step*−*scan* procedure.

The electron energy in the mass spectrometer is set to 70 eV, where the ionization cross sections usually have their maximum. Specific species can only be identified in a mass spectrum, if one takes their cracking pattern into account. In our case, this requirement is relaxed for the discussion of larger hydrocarbons since it is possible to select mass peaks, where only one species preferentially contributes. This is different for smaller hydrocarbons, since many species with higher mass may contribute to a single mass channel at lower mass. In such a case, we use more a elaborate method to analyze the spectra in a quantitative manner, which is based on Bayes statistics.[15,16] These results will be published elsewhere.[17]

Additionally, the influence of acetone on the measurement is investigated. Acetone is commonly used as a solvent for acetylene and by feeding acetylene to the plasma, a small fraction of acetone is able to reach the reactor, which shows up in the mass spectra. In order to check the influence of acetone on the plasma chemistry, some measurements are repeated with acetone free acetylene. These experiments show a reduced signal of H_2(40% lower), CH_4 (40%), and CO (30%) compared to the case when acetylene diluted in acetone is used. However, no significant change in the plasma composition regarding bigger hydrocarbon molecules are observed.

Results and Discussion

The time evolution of the most intense signals measured at masses of 2, 26, and 50 amu is shown in Figure 2b. Mass 26 amu corresponds to C_2H_2 molecules. Since it is the precursor gas, its signal is large prior to plasma ignition and decreases sharply after plasma ignition due to plasma induced C_2H_2 consumption. After several seconds, an equilibrium between gas flow into the reactor and the losses inside the plasma volume via electron impact dissociation and via pumping is reached. The signal at mass 2 amu corresponds to molecular hydrogen (H_2). It is also measured prior to plasma ignition, as a part of the cracking pattern of C_2H_2 and of the background gas inside the mass spectrometer. The signal at mass 2 amu increases after plasma ignition indicating H_2 production in the plasma. It is very large, but this is a consequence of a discrimination of heavy species in the quadrupole mass spectrometer relative to light ones. Indeed, the signal prior to plasma ignition at mass 2 amu is already 100 000 c/s. The actual H_2 density in the reactor is expected to be much lower than the C_2H_2 density at all times. Additionally, the background density of hydrogen in the mass spectrometer can vary, since it is produced in electron collisions with various hydrocarbon molecules and via pyrolysis of these molecules on the hot filament in the ionizer of the mass spectrometer. Therefore, the H_2 measurement at mass 2 amu should be only considered as a very rough estimation of the H_2 relative density change in time. We have not performed any

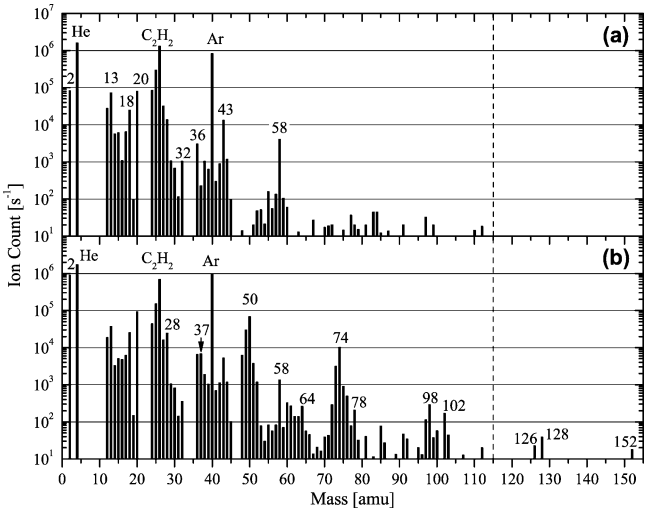

Figure 3. Reconstructed neutral mass spectra according to the step-scan procedure before plasma ignition (a) and 1 second after plasma ignition (b).

detailed analysis of the signal at mass 2 amu due to these reasons. The signal at mass 50 amu corresponds to the parent peak of diacetylene molecules (C_4H_2). C_4H_2 is a reaction product in the plasma, because it is not detected prior to plasma ignition. The signal at mass 50 amu goes through a maximum 0.7 s after plasma ignition and decreases again, following approximately the depletion of acetylene. The gas flow of acetylene is turned off at $t = 8$ s, resulting in the drop of the signals at all masses shown in Figure 2b, caused by fast dissociation of these molecules in the still running Ar/He plasma. The delay of approximately 1 second is due to gas in the gas line between mass flow controller and reactor. The variation of the intensities depicted in Figure 2b results mainly from the rapidly evolving plasma chemistry including the formation and presence of nanoparticles (with diameter up to 28 nm.[7]) Figure 3 shows two mass spectra generated via the step-scan procedure at times just prior and 1 second after plasma ignition. The mass peaks corresponding to Ar (mass 20, 36, 38, and 40 amu), He (4), and C_2H_2 (12, 13, and 24−26 amu) are visible in the first spectrum together with peaks for acetone (15, 43, and 58 amu) and H_2 (2 amu). Weak signals of background gases N_2 (28 amu), O_2 (32 amu) and H_2O (16−18 amu) are present as well. Some very weak signals at masses above 60 amu (e.g., masses 67, 83, or 84 amu) are due to a background atmosphere in the mass spectrometer. The signal at these masses stays constant during the whole process. Dramatic changes in the gas composition can be seen in Figure 3b taken at 1 s after plasma ignition. The consumption of acetylene is accompanied by an increase and an appearance of new peaks corresponding to various hydrocarbons. (For example, peaks originating from the cracking pattern of C_4H_2 appears at masses 37, 48, 49, and 50 amu; C_6H_2 at masses 72, 73, and 74 amu; or C_8H_2 at masses 97 and 98 amu.) One can clearly see that hydrocarbons with even numbers of carbon atoms are preferentially formed since the signal at masses 60 to 64 amu is rather small. These mass spectra correspond qualitatively as well as quantitatively (relative peak heights are comparable) very well to the results measured by Deschenaux[10] in pure C_2H_2 discharges, indicating that the addition of noble gases to a C_2H_2 plasma does not alter much its plasma chemistry. Consequently, we assume that the positive and negative ion spectra, as measured by Deschenaux et al.,[9] are also representative for our plasma.

Qualitative Analysis of the Plasma Polymerization of C_2H_2. Unsaturated hydrocarbon molecules with mainly triple

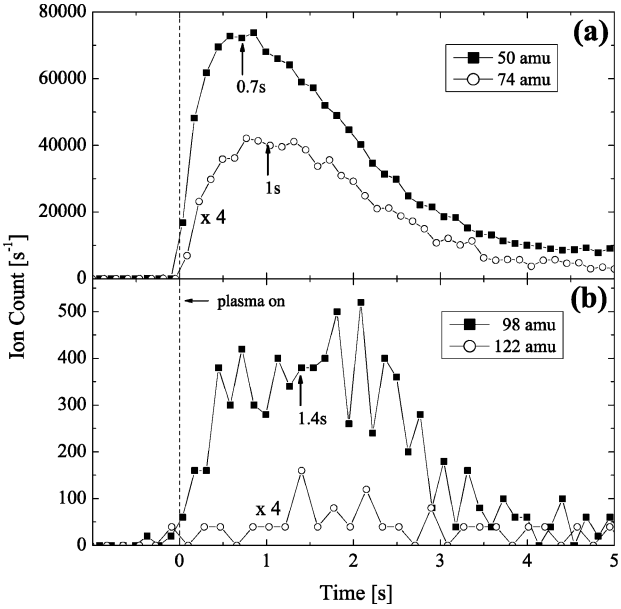

Figure 4. Temporal evolution of signals corresponding to parent masses of C_4H_2 (50 amu), C_6H_2 (74 amu), C_8H_2 (98 amu), and $C_{10}H_2$ (122 amu). The arrows indicate the estimated position of signal maxima.

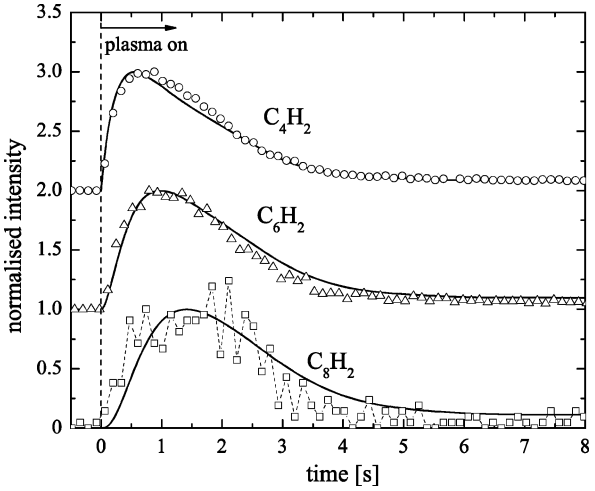

Figure 5. Comparison of normalized temporal evolution of signals (symbols) corresponding to parent masses of C_4H_2 (50 amu), C_6H_2 (74 amu), and C_8H_2 (98 amu) with the behavior (full lines) predicted by a simple chemistry model (see text). The data points and curves for C_4H_2 and C_6H_2 are shifted for clarity.

bonds and masses above 45 amu are well characterized by their signal at the parent mass, since the contribution from cracking patterns of other triple bonded hydrocarbons is negligible. This is different for smaller hydrocarbons with masses below 46 amu, where an intimate overlap of the cracking patterns needs to be taken into account prior to decomposing the mass spectra. The results of the Bayesian analysis,[17] not presented here, confirms that the peaks of the parent mass are well suited to analyze the temporal evolution of these species densities.

$C_{2n}H_2$ Molecules. Figure 4 shows signals measured at masses of 50, 74, 98, and 122 amu corresponding to $C_{2n}H_2$ ($n = 2-5$) molecules. Possible contributions from the cracking patterns of C_nH_4 species can be neglected, due to their very low densities and their negligible contribution to the measured signals. $C_{2n}H_2$ ($n = 2-5$) molecules are formed via polymerization reactions induced by C_2H radicals, which are formed in electron impact dissociation of the source gas C_2H_2:[18]

$$C_2H_2 + e^-(E_{el} \geq 7.5\ eV) \rightarrow C_2H + H + e^- \qquad (1)$$

Polymerization proceeds through consecutive steps via addition of C_2H radicals to $C_{2n}H_2$ molecules, starting with acetylene:

$$C_{2n}H_2 + C_2H \rightarrow C_{2n+2}H_2 + H \qquad (2)$$

This polymerization sequence induces delays between the appearance of the maximum intensities of the species involved as indicated by arrows in Figure 4. The positions of these maxima are estimated based on the signal heights and symmetry and similarity of the profiles. The spectrum of $C_{10}H_2$ is close to the detection limit and too noisy to estimate the position of the signal maximum. The first polymerization step involving C_2H_2 molecules and C_2H radicals was well studied in the past.[19] It has a rate constant of $k_2 = 1.3 \times 10^{-10}$ cm^3 s^{-1} with C_4H_2 being the dominant product. The rate constants of the consecutive polymerization steps are not known, but the similar delay of 0.3−0.4 s between the appearance of the maxima in Figure 3 indicates, that the rate constants are comparable to k_2. However, one can expect, that the probability that a C_2H radical will bound to one of the end carbon atoms will decrease with increasing length of the molecule involved in reaction 2. As a consequence, the formation of branched $C_{2n}H_2$ radicals becomes a viable reaction route besides the formation of linear molecules. The signal at mass 98 amu, where the parent peak of linear C_8H_2 molecule is located, is quite small, suggesting that such branching may cause a limited production of linear C_8H_2 molecules. More accurate statement can only be made after quantitative analysis of our results, which will be performed by means of Bayes statistics and will be published in our future article.[17] To confirm, that C_2H induced chain polymerization of acetylene is a plausible explanation for formation of the $C_{2n}H_2$ ($n = 2-4$) molecules, we have constructed a simple chemistry model (cf. Appendix). Normalized signal intensities of the model results and MS measurements are shown in Figure 5 and show very good agreement, confirming that the proposed reaction scheme is correct. The C_6H^- (normalized intensity 100%), $C_6H_2^-$ (10%), $C_8H_2^-$ (7%), and C_4H^- (6%) are the anions with the highest signal in the negative ion mass spectrum of Deschenaux et al. The $C_{2n}H_2$ molecules are probable precursors of these anions, which are created in DEA reactions such as

$$C_{2n}H_2 + e^- \rightarrow C_{2n}H^- + H(n > 1) \qquad (3)$$

The feasibility of this reaction scheme depends strongly on the reaction constants of these DEA reactions, which are unfortunately not known. However, it is conceivable to assume that the rate constants increase with the possible vibrational excitation of the $C_{2n}H_2$ molecules, as discussed by Christophorou[20] and as it is known for example from rate constant of DEA of H_2 with increase of several orders of magnitude.[21] The model of de Bleecker et al. has shown that high signals of, e.g., C_6H^- and C_4H^- compared to C_2H^- cannot be reproduced when only reaction 3 with ground state acetylene ($n = 1$), followed by polymerization with C_2H_2, is included in the model as a source of $C_{2n}H^-$ anions. The reaction scheme we propose might explain this discrepancy.

$C_{2n}H_4$ Molecules. Figure 6 shows signals measured at masses of 52, 64, and 76 amu corresponding to C_nH_4 ($n = 4-6$) molecules. The contribution of C_4H_2 and C_6H_2 to masses 52 and 76 amu due to the natural abundance of the ^{13}C isotope is below 5%. The signals measured at mass 50 amu (C_4H_2) and mass 74 amu (C_6H_2) are rescaled and plotted in this figure for comparison. The signal intensities at the parent masses of C_nH_4

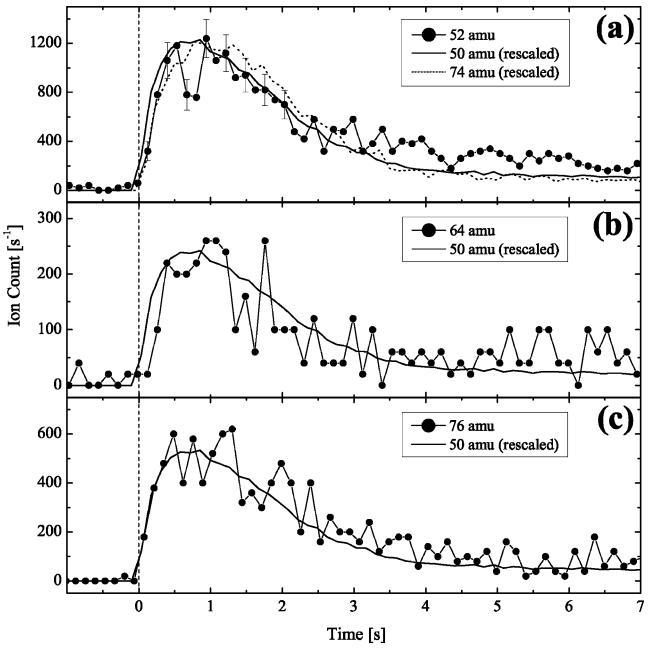

Figure 6. Time evolution of the signal corresponding to parent masses of C_4H_4 [52 amu (a)], C_5H_4 [64 amu (b)] and C_6H_4 [76 amu (c)]. The rescaled signals at mass 50 and 76 amu are also shown for comparison.

species are much lower than those of $C_{2n}H_2$ species indicating their very low densities. The signal at mass 64 amu corresponding to C_5H_4 molecules is the lowest, indicating, that the production of molecules with odd number of carbon atoms is again suppressed. Because of the unknown cracking patterns of these molecules, no better statement regarding their absolute densities can be made at this point. Moreover, contrary to $C_{2n}H_2$ species, where only one configuration is possible for each molecule, more isomers can be subscribed to each C_nH_4 molecule. Similar to $C_{2n}H_2$, the signals for C_nH_4 reach their maximum after plasma ignition and decrease again due to the depletion of the precursor gas. In order to reveal the pathway leading to the formation of these species, the measured signals are compared to the measurements at masses 50 and 74 amu. Figure 5a clearly shows, that C_4H_4 exhibits a very similar temporal evolution as C_4H_2 and that the maximum of the signal at mass 52 amu appears prior to the maximum of C_6H_2. This suggests that $C_{2n}H_2$ ($n = 2, 3, 4, ...$) species are not involved in the formation of C_4H_4, since the necessary hydrogen insertion in, e.g., C_4H_2 to form C_4H_4 would cause a delay in the appearance of signal maxima of C_4H_4, in a similar way as it is observed for C_6H_2.

Additionally, the relative abundance of C_4H_4 (and also of C_5H_4 and of C_6H_4) compared to C_4H_2 is higher at 3 s after the plasma ignition and beyond. At this moment C_2H_2 is already depleted and the plasma is dominated by the presence of molecular hydrogen (cf. Figure 2). In this case, hydrogen insertion might be causing the production of C_4H_4. But how is the production of C_4H_4 at the initial stage of the experiment possible without involvement of C_2H radicals? As a hypothesis, we propose two possible reactions: (i) a reaction of acetylene with vinylidene or (ii) the mutual neutralization reaction of anions and cations.

(i) Reaction of Acetylene with Vinylidene: Vinylidene is a metastable isomer of acetylene lying approximately 2 eV (singlet) and 4 eV (triplet) above the ground state.[22] The triplet state of vinylidene has a lifetime of 5 μs,[23] and the rearrangement barrier to acetylene is larger than 2.2 eV.[22] Vinylidene is a biradical, which easily reacts in collisions with acetylene or molecular hydrogen forming hydrogen rich hydrocarbons. Since the electron temperature in low-pressure plasmas is usually lying between 2 and 5 eV, the formation of metastable vinylidene in inelastic collision with an electron is probable:

$$HC{\equiv}CH + e^- (E_{el} \geq 6.2eV) \rightarrow H_2C{=}C + e^- \qquad (4)$$

It is most likely that vinylidene is involved in the pyrolysis of acetylene at 400−900 °C with C_4H_4 and C_6H_6 being the only detected products.[24] In addition vinylidene presence in microwave plasmas from acetylene is indicated by MS measurements of Fujii.[25] A possible reaction sequence for C_4H_4 production from vinylidene is

$$H_2CC + C_2H_2 \rightarrow C_4H_3 + H \qquad (5)$$

$$C_4H_3 + H_2 \rightarrow C_4H_4 + H \qquad (6)$$

We restrict us here only to *two-to-two* reactions, since we expect that the direct formation of C_4H_4 in *two-to-one* reaction of vinylidene with acetylene is unlikely due to the absence of collisional stabilization of reaction products at low pressures. Unfortunately, the reaction rate of reactions 4−6 are not known in order to test the plausibility of this proposal. Any experimental detection of vinylidene by threshold ionization mass spectrometry cannot be easily realized due to its short lifetime leading to a deexcitation on the way between plasma and mass spectrometer.

(ii) Mutual Neutralization Reaction of Anions and Cations: Another possible formation path for C_nH_4 species occurs via mutual neutralization reactions of anions and cations. The measurements of Deschenaux et al.[9] reveal the presence of $C_2H_2^+$, $C_4H_2^+$, $C_4H_3^+$, or $C_6H_2^+$ cations and H_2CC^-, C_4H^-, or C_6H^- anions. The anion at mass 26 amu is most probably the vinylidene anion H_2CC^-, since the acetylene anion itself is unstable with respect to autodetachment. The vinylidene anion is more stable compared to the vinylidene neutral (collisionless lifetime longer than 100 s) and therefore stable with respect to autodetachment.[22] The exact reaction pathway leading to the formation of vinylidene anions is not known. However, it is conceivable that it is formed in the plasma very quickly, since it is observed in the negative ion spectra measured by Deschenaux et al.:[9] in their pulsed CCP plasma modulated with a frequency of 500 Hz, the signal intensity at mass 26 amu is 20 times higher than at mass 25 amu for C_2H^- (a product of dissociative electron attachment to acetylene). The mutual neutralization is very fast due to Coulomb interaction with rate constants 3 orders of magnitude larger than in the case of neutral reactants.[11,26] We can estimate the production rate of the C_nH_4 molecules by taking the positive ion and vinylidene anion densities of 2×10^{14} m^3 and 2×10^{16} m^3 respectively (based on the model results of de Bleecker et al.) and taking into account 1000 times faster reaction rate of mutual neutralization reaction compared to, for example, the neutral−neutral reaction of acetylene (10^{20} m^3) with the C_2H radical (10^{16} m^3). The production of the C_nH_4 molecules in the reactions

$$H_2CC^- + C_{2(4)}H_2^+ \rightarrow C_{4(6)}H_3 + H \qquad (7)$$

(followed again by hydrogen insertion), is approximately 250 times slower than C_4H_2 production but it could be still a plausible source of these minority C_nH_4 molecules. The C_4H_4 and C_6H_4 can be also produced directly in neutralization reactions:

$$H_2CC^- + C_4H_3^+ \rightarrow C_{6(4)}H_4 + (C_2)H \qquad (8)$$

The presence of C_nH_4 species is an indicator that vinylidene and/or mutual neutralization reactions involving vinylidene anions can play an important role in the plasma chemistry. On the other hand, the densities of C_nH_4 molecules are probably too low to play any significant role in the dust particle nucleation.

Aromatic Compounds. Figure 7 shows signals measured at masses 78 (C_6H_6) and 102 amu (C_8H_6). The rescaled signal at mass 50 amu is included again for comparison. The aromatic compounds benzene and phenylacetylene are expected to be the main contributors to these signals. Because of the complexity of the mass spectra and the low level of the signals it could not be directly tested, whether other isomers are present in the gas phase as well. However, aromatic compounds are the most stable isomers[27] and they are often observed in acetylene pyrolysis or combustion.[24,28] The presence of peaks at masses 126, 128, and 152 amu (cf. Figure 3b) indicates the presence of diethynylbenzene, naphthalene and ethynylnaphthalene/acenaphthylene respectively, products of the hydrogen abstraction/acetylene addition (HACA) mechanism, which accounts for their generation after the first aromatic ring is formed.[28] Therefore, we believe, that the peaks at masses 78, 102, 126, 128, and 152 amu are parent peaks of aromatic compounds mentioned above. The comparison with the C_4H_2 signal in Figure 7 shows that the C_6H_6 maximum density appears later than that of C_4H_2, and therefore also that of C_4H_4. Moreover, as in the case of C_nH_4 species, the relative intensity compared to C_4H_2 is clearly higher at 3 s after plasma ignition and beyond. The formation of the initial aromatic rings is still a topic of scientific debate. In the model of De Bleecker et al.[12] 75,3% of benzene is produced via addition of acetylene to C_4H_3 and 25.7% via C_6H_4 cyclization. The appearance of C_6H_6 after C_4H_4 is in agreement with the reaction identified in this model. However, as mentioned above, the formation of C_4H_3 occurs probably via reactions (eq 5) involving vinylidene or mutual neutralization (eq 7). The signal measured at mass 102 amu exhibits a very rapid increase after plasma ignition compared to other masses, cf. Figure 7b. Such a fast increase of the signal cannot be explained by gas-phase polymerization reactions. Instead it is observed that the cleaning of the reactor using an Ar/O_2 plasma prior the acetylene experiments resulted in a much slower signal buildup, as shown in Figure 8. Moreover, the amount of phenylacetylene depends on the number of particle generation experiments (*steps*) prior to the actual mass spectrometry measurements, since the signal increases when more deposition/particle generation steps precede the measurement. These observations are an evidence that surface reactions occur, most probably between C_2H radicals and surface bonded or adsorbed aromatic rings:

$$C_6H_{5(6)}|_{surface} + C_2H|_{plasma} \rightarrow C_8H_6|_{plasma}(+H) \qquad (9)$$

The measurements at mass 102 amu show, that surface reactions may play an important role in the formation of larger aromatic compounds under the low-pressure acetylene plasma conditions. The time-resolved measurements at masses 126, 128, and 152 amu are not shown, since the signals are very weak with a poor signal-to-noise ratio. Aromatic compounds are involved in the nucleation process of soot particles in combustion.[28] Therefore, they may also be important precursor of dust particles in our plasma as well. However, the very low signals at the masses of their parent peaks imply their very low densities in comparison to $C_{2n}H_2$ molecules. Moreover, anions with only one or two

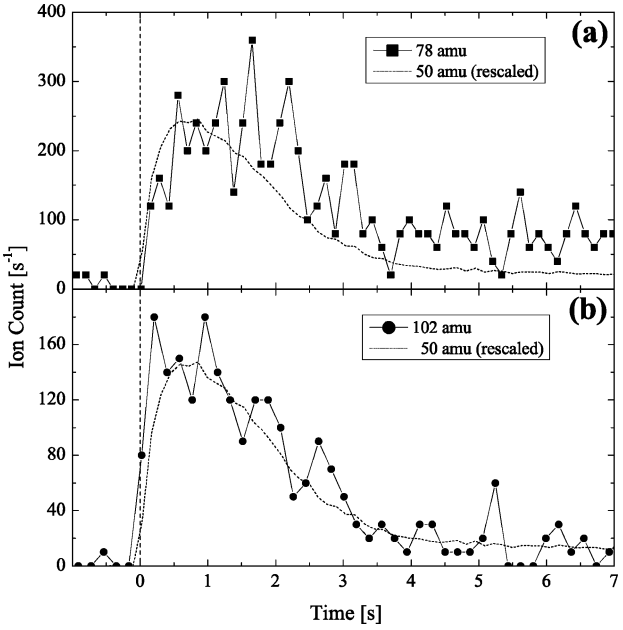

Figure 7. Temporal evolution of signals corresponding to parent masses of C_6H_6 [78 amu (a)] and C_8H_6 [102 amu (b)]. The rescaled signal at mass 50 amu is also shown for comparison.

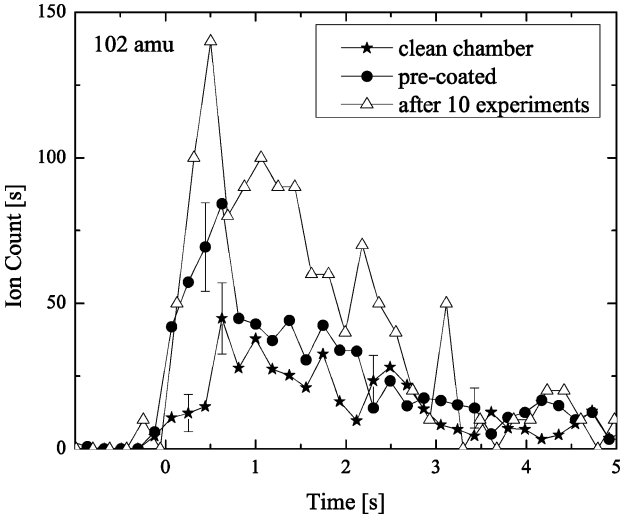

Figure 8. Temporal evolution of mass 102 amu with a clean and a pre-coated (after one experiment using 30 s of C_2H_2 injection in the plasma) reactor. Every curve is an average of three mass spectrometry measurements. The data taken after 10 experiments with conditions as described in the text is a single mass scan.

hydrogen atoms were mainly observed,[9] excluding aromatic compounds from being the precursors for their formation. Therefore, we believe that aromatic compounds play only a minor role in particle formation under our experimental conditions.

Conclusions

The temporal evolution of neutral species in a capacitively coupled plasma from argon, helium and acetylene is followed via molecular beam mass spectrometry in a qualitative manner. The following species and chemistry pathways are identified: (i) The formation of $C_{2n}H_2$ species proceeds through the C_2H-induced polymerization of the C_2H_2 monomer. (ii) It is shown, that C_nH_4 species do not result from the hydrogenation of $C_{2n}H_2$ molecules. Two possible alternatives involving vinylidene or mutual neutralization are proposed instead. (iii) C_6H_6 can be

formed via addition of acetylene to C_4H_3 or via C_6H_4 cyclization as proposed by de Bleecker et al.[12] However, C_4H_3 and C_6H_4 precursors are probably formed as described in point ii. (iv) A surface reaction is responsible for the formation of C_8H_6 (phenylacetylene) suggesting, that surface reactions can be a significant source of aromatic compounds in low-pressure acetylene plasmas. As already mentioned, it is believed that dust particle growth proceeds through the growth of negative ions trapped in the plasma. On the basis of our results we propose that $C_{2n}H_2$ molecules ($n > 1$) are an important precursor for fast formation of these negative ions and hence play an important role in dust particle formation.

Appendix

A simple zero-dimensional plug-down chemistry model is constructed to predict the time evolution of $C_{2n}H_2$ ($n = 2-4$) densities (n_{2n} in the equations below) in the first 8 seconds after plasma ignition. For every species a differential equation is written:

$$\frac{dn_4}{dt} = n_{C_2H_2} n_{C_2H} k_{2\to4} - n_4 n_{C_2H} k_{4\to6} - n_4 n_e k_{diss} - n_4/\tau \quad (10)$$

$$\frac{dn_6}{dt} = n_4 n_{C_2H} k_{4\to6} - n_6 n_{C_2H} k_{6\to8} - n_{46} n_e k_{diss} - n_6/\tau \quad (11)$$

$$\frac{dn_8}{dt} = n_{C_2H} k_{6\to8} - n_8 n_{C_2H} k_{8\to10} - n_8 n_e k_{diss} - n_8/\tau \quad (12)$$

Additionally, a differential equation for C_2H radical density is used in the form:

$$\frac{dn_{C_2H}}{dt} = n_{C_2H_2} n_e k_{diss} - n_{C_2H}\{n_{C_2H_2} k_{2\to4} + n_4 k_{4\to6} + n_6 k_{6\to8} + n_8 k_{8\to10}\} \quad (13)$$

All densities are set to zero at time zero as an initial condition. The following assumptions are used: (i) the reaction rates $k_{4\to6}$, $k_{6\to8}$, and $k_{8\to10}$ for the chain polymerization reactions are set to the known value of $k_{2\to4}$ of 1.3×10^{-10} cm^3 s^{-1};[19] (ii) the acetylene density $n_{C_2H_2}$ in the first 8 s of the plasma is parametrized by the measured signal at mass 26 amu with the initial density prior to plasma ignition obtained from the partial pressure of acetylene; (iii) the residence time of the neutral species in the reactor τ is set to 4.9 s and (iv) the $n_e k_{diss}$ product, which takes into account the dissociation of species in collisions with energetic electrons, is assumed to be the same for all species and constant during the complete process. the $n_e k_{diss}$ product is used as a fitting parameter (optimal value of 1.4 s^{-1}) to obtain a good fit between modeled and measured profiles. The set of differential eqs 10−13 is solved using COMSOL Multiphysics 3.2 software.

Acknowledgment. The authors thank Norbert Grabkowski for his skillful technical assistance. The work is supported by the German Science Foundation in the framework of the graduate school 1051 and the coordinated research center 591.

References and Notes

(1) Bouchoule, A. *Dusty Plasmas: physics, chemistry and technological impacts in plasma processing*; John Wiley & Sons: New York, 1999.
(2) Hollenstein, C. *Plas. Phys. Contr. Fusion* **2000**, *42*, R93.
(3) Kortshagen, U.; Mangolini, L.; Bapat, A. J. *Nanopart. Res.* **2007**, *9*, 39.
(4) Winter, J. Private communication.
(5) Longeaud, C.; Kleider, J. P. R. i Cabarrocas, S. Hamma, R. Meaudre, and Meaudre, M. *J. Non.-Cryst. Solids* **1998**, *96*, 227−230.
(6) Schulze, M.; von Keudell, A.; Awakowicz, P. *Appl. Phys. Lett.* **2006**, *88*, 141503.
(7) Schulze, M.; von Keudell, A; Awakowicz, P. *Plasma Sources Sci. Technol.* **2006**, *15*, 556.
(8) Schulze, M.; von Keudell, A.; Awakowicz, P. Unpublished work.
(9) Deschenaux, C.; Affolter, A.; Magni, D.; Hollenstein, C.; Fayet, P. *J. Phys. D.* **1999**, *32*, 1876.
(10) Deschenaux, C. Ph.D. Thesis, École Polytechnique Fédérale de Lausanne, Lausanne, Switzerland, 2002.
(11) Bleecker, K. D.; Bogaerts, A.; Goedheer, W. *Phys. Rev. E.* **2006**, *73*, 026405.
(12) Bleecker, K. D.; Bogaerts, A.; Goedheer, W. *Appl. Phys. Lett.* **2006**, *88*, 151501.
(13) Sorokin, M.; Kroesen, G. M. W.; Stoels, W. W. *IEEE Trans. Plasma Sci.* **2004**, *32*, 731.
(14) van den Donker, M. N.; Rech, B.; Finger, F.; Kessels, W. M. M.; and van de Sanden, M. C. M. *Appl. Phys. Lett.* **2005**, *87*, 263503.
(15) Schwarz-Selinger, T.; Preuss, R.; Dose, V.; von der Linden, W. *J. Mass Spectrom.* **2001**, *36*, 866.
(16) Kang, H.; Preusss, Schwarz-Selinger, R. T.; Dose, V. *J. Mass Spectrom.* **2002**, *37*, 748.
(17) Consoli, A.; Benedikt, J.; Schulze, M.; von Keudell, A. To be published.
(18) Janev, R.; Reiter, D. *Phys. Plasmas* **2004**, *11*, 780.
(19) Laufer, A. H.; Fahr, A. *Chem. Rev.* **2004**, *104*, 2813.
(20) Christophorou, L. G. *Environ. Health Perspect.* **1980**, *36*, 3.
(21) Wadehra, J. M.; Bardsley, J. N. *Phys. Rev. Lett.* **1978**, *41*, 1795.
(22) Ervin, K.; Ho, J.; Lineberger, W. *J. Chem. Phys.* **1989**, *91*, 5974.
(23) Levin, J.; Feldman, H.; Baer, Ben-Hamu, A. D.; Heber, O.; Zajfman, D.; Vager, Z. *Phys. Rev. Lett.* **1998**, *81*, 3347.
(24) Xu, X.; Pacey, P. *Phys. Chem. Chem. Phys.* **2001**, *3*, 2836.
(25) Fujii, T. *Phys. Rev. E.* **1998**, *58*, 6495.
(26) Hickman, A. *J. Chem. Phys.* **1979**, *70*, 4872.
(27) Stein, S.; Fahr, A. *J. Phys. Chem.* **1985**, *89*, 3714.
(28) Richter, H.; Howard, J. B. *Prog. Energy Combust. Sci.* **2000**, *26*, 565.